Am J Physiol Heart Circ Physiol 307: H945–H957, 2014.
First published July 25, 2014; doi:10.1152/ajpheart.00918.2013.

Poldip2 controls vascular smooth muscle cell migration by regulating focal adhesion turnover and force polarization

Srinivasa Raju Datla,[1] Daniel J. McGrail,[2] Sasa Vukelic,[1] Lauren P. Huff,[1] Alicia N. Lyle,[1] Lily Pounkova,[1] Minyoung Lee,[1] Bonnie Seidel-Rogol,[1] Mazen K. Khalil,[1] Lula L. Hilenski,[1] Lance S. Terada,[4] Michelle R. Dawson,[2,3] Bernard Lassègue,[1] and Kathy K. Griendling[1]

[1]*Department of Medicine, Division of Cardiology, Emory University School of Medicine, Atlanta;* [2]*Department of Chemical and Biomolecular Engineering and* [3]*The Petit Institute for Bioengineering and Bioscience, Georgia Institute of Technology, Atlanta, Georgia;* [4]*Department of Internal Medicine, Division of Pulmonary and Critical Care, University of Texas Southwestern Medical Center, Dallas, Texas*

Submitted 25 November 2013; accepted in final form 22 July 2014

Datla SR, McGrail DJ, Vukelic S, Huff LP, Lyle AN, Pounkova L, Lee M, Seidel-Rogol B, Khalil MK, Hilenski LL, Terada LS, Dawson MR, Lassègue B, Griendling KK. Poldip2 controls vascular smooth muscle cell migration by regulating focal adhesion turnover and force polarization. *Am J Physiol Heart Circ Physiol* 307: H945–H957, 2014. First published July 25, 2014; doi:10.1152/ajpheart.00918.2013.—Polymerase-δ-interacting protein 2 (Poldip2) interacts with NADPH oxidase 4 (Nox4) and regulates migration; however, the precise underlying mechanisms are unclear. Here, we investigated the role of Poldip2 in focal adhesion turnover, as well as traction force generation and polarization. Poldip2 overexpression (AdPoldip2) in vascular smooth muscle cells (VSMCs) impairs PDGF-induced migration and induces a characteristic phenotype of long cytoplasmic extensions. AdPoldip2 also prevents the decrease in spreading and increased aspect ratio observed in response to PDGF and slightly impairs cell contraction. Moreover, AdPoldip2 blocks focal adhesion dissolution and sustains H_2O_2 levels in focal adhesions, whereas Poldip2 knockdown (siPoldip2) significantly decreases the number of focal adhesions. RhoA activity is unchanged when focal adhesion dissolution is stimulated in control cells but increases in AdPoldip2-treated cells. Inhibition of RhoA blocks Poldip2-mediated attenuation of focal adhesion dissolution, and overexpression of RhoA or focal adhesion kinase (FAK) reverses the loss of focal adhesions induced by siPoldip2, indicating that RhoA and FAK mediate the effect of Poldip2 on focal adhesions. Nox4 silencing prevents focal adhesion stabilization by AdPoldip2 and induces a phenotype similar to siPoldip2, suggesting a role for Nox4 in Poldip2-induced focal adhesion stability. As a consequence of impaired focal adhesion turnover, PDGF-treated AdPoldip2 cells are unable to reduce and polarize traction forces, a necessary first step in migration. These results implicate Poldip2 in VSMC migration via regulation of focal adhesion turnover and traction force generation in a Nox4/RhoA/FAK-dependent manner.

polymerase-δ-interacting protein 2; NADPH oxidase 4; focal adhesions; vascular smooth muscle cells; cytoskeleton; traction forces; reactive oxygen species

CELL MIGRATION PLAYS A CENTRAL ROLE in multiple biological phenomena. During embryogenesis, it is critically important for morphogenesis; in the adult organism, it is involved in the inflammatory response and the wound-healing process. However, cell migration also has untoward effects in many disease processes, including inflammatory cell migration in arthritis, endothelial cell migration in cancer angiogenesis, and smooth muscle cell migration in restenosis and atherosclerosis.

During migration, slow-moving cells undergo cyclic structural alterations and typically form a leading migratory front (the lamellipodium) and a retracting tail, collectively generating a polarized cell shape. Lamellipodial formation is initiated by protrusion of actin filaments in the direction of the chemotactic stimulus (24). Formation of focal adhesions, which act as anchoring points to the extracellular matrix (ECM), stabilizes lamellipodial extensions (45). Conversely, dissolution of focal adhesions at the trailing end of the cell is required for retraction of the tail (24). This spatially ordered assembly and disassembly of focal adhesions promotes the front-to-rear polarity of the migrating cell (2, 9, 15, 33). Changes in intracellular force distribution are transmitted as traction forces to the extracellular matrix by focal adhesions, which are located at the ends of actin bundles (50). During the migratory process, release of rear focal adhesions subsequently decreases these traction forces in the back of the cell. Therefore, the distribution of local forces over the whole cell becomes polarized, as the center of traction force moves forward relative to the geometric cell center (26). Polarization of traction forces is a consequence of both the strength of focal adhesions and the activity of myosin II on actin fibers (38).

We recently showed that the NADPH oxidase 4 (Nox4), along with its interacting partner polymerase-δ-interacting protein 2 (Poldip2), is expressed in focal adhesions and mediates vascular smooth muscle cell (VSMC) migration (27) but did not determine what part of the migratory cycle is targeted by this complex. We did report that Poldip2 overexpression induces a sustained increase in the activity of the small GTPase RhoA (27). Previous work, mostly in fibroblasts, has shown that spatiotemporally precise activation and inactivation of RhoA (40) promotes migration by inducing actin filament bundling and the clustering of integrins and associated proteins into focal adhesion complexes (28, 41, 44), by regulating focal adhesion kinase (FAK)-dependent focal adhesion dissolution (35), and by controlling cell body contraction via Rho kinase-mediated inhibition of myosin light chain phosphatase (47). RhoA can thus affect multiple aspects of migration when it properly cycles through its active and inactive states, but whether it mediates the effects of Poldip2/Nox4 and which of its functions are affected by Poldip2/Nox4 remain unclear.

In this study, we tested the hypothesis that Poldip2 induction of Rho impairs VSMC migration primarily by regulating focal adhesion dissolution and cell polarization. We found that in

Address for reprint requests and other correspondence: K. Griendling, Emory Univ., Division of Cardiology, 101 Woodruff Circle, WMB 308, Atlanta, GA 30322 (e-mail: kgriend@emory.edu).

fact Poldip2, via activation of RhoA/FAK, inhibits focal adhesion dissolution, sustains H_2O_2 levels in focal adhesion, and is required for focal adhesion formation. These coordinated effects on focal adhesion turnover prevent polarization of traction forces and thereby impair migration following Poldip2 overexpression. We not only identify for the first time the biological basis of Poldip2-mediated effects on focal adhesion turnover but also identify RhoA/FAK as biologically relevant targets of Poldip2/Nox4, which may prove valuable in the development of more specific antimigratory therapeutics.

MATERIALS AND METHODS

Cell culture. Rat aortic VSMCs (*passages 7–12*) were grown in Dulbecco's Modified Eagle's Media (DMEM) as described previously (27).

Antibodies. Nox4 antibodies were kindly provided by Dr. David Lambeth (Emory University). Poldip2 goat antibody was custom made by GenScript (Piscataway, NJ) against the peptide sequence NPAGHGSKEVKGKTC, as reported previously (27). When available, the following commercial antibodies were used: FAKpY397 and paxillin (BD Bioscience, San Jose, CA or Abcam, Cambridge, MA), Myc (Cell Signaling, Billerica, MA), total FAK (EMD Millipore, Billerica, MA), tubulin and HA-tag (Abcam), and CDK4 (Santa Cruz Biotechnology, Santa Cruz, CA). Secondary antibodies were from Jackson ImmunoResearch (West Grove, PA) or Bio-Rad (Hercules, CA).

siRNA. For transfection with siRNA, VSMCs were trypsinized and plated at 40–50% confluence on collagen-coated cover slips or 100-mm cell culture dishes. After 4 h, cells were washed with serum-free Opti-MEM and incubated with siRNA and Oligofectamine complexes for 48 h. Cells were incubated in OPTI-MEM for an additional 2–4 days (12, 27). A stealth siRNA against human, mouse, and rat Poldip2 (siPoldip2; sense: 5′GCCCACAUAUAUCUCAGAGAUCUCA3′, antisense: 5′UGAGAUCUCUGAGAUAUAUGUGGGC3′) and the stealth control siRNA (siControl) of the corresponding GC content were purchased from Invitrogen (Carlsbad, CA). Cells were transfected with a final siRNA concentration of 15 nmol/l. Nox4 siRNA (siNox4; 25 nmol/l) was used as described previously, with the Allstars Negative Control (Qiagen, Valencia, CA) (12, 27).

Adenoviruses. The AdEasy System was used to prepare viruses with either no insert (green fluorescent protein-expressing adenovirus, AdGFP, control for AdPoldip2), or NH_2-terminal-Xpress-tagged and C00H-terminal-myc-tagged Poldip2 [AdPoldip2, which also includes GFP driven by an independent cytomegalovirus (CMV) promoter]. The LacZ control (AdLacZ, control for AdRhoGV and AdFAK) and HA-tagged constitutively active RhoA (AdRhoGV) adenoviruses were kind gifts of Dr. Aviv Hassid (University of Tennessee). The FAK-overexpressing adenovirus (AdFAK) was a kind gift from Dr. Joseph C. Loftus (Mayo Clinic, Phoenix, AZ). VSMCs were transduced with recombinant adenoviruses for 2 h at 37°C in serum-free DMEM, followed by incubation for 48 h to 3 days in serum-free DMEM without virus (12, 27).

Wound-healing assay. The wound-healing assay was performed as described previously (13). Rat aortic VSMCs were seeded on MatTek (Ashland, MA) dishes treated with adenovirus in serum-free media. Three days after transduction, when cells had reached 100% confluence, a wound was made using a pipette tip, and detached cells were removed. Cells were then stimulated with PDGF (10 ng/ml) in serum-free DMEM, and live cell images were acquired with a Leica TCS SP5 II confocal microscope system equipped with an environmental chamber using a ×20 air objective lens (NA = 0.70) and LAS AF software. Images were taken every 15 min for 18 h. In some cases, the cells were grown on collagen-coated coverslips and fixed at indicated time points. Nuclei were stained with DAPI. GFP fluorescence was used as an indicator of transduced cells. Fixed cell images were acquired with an Olympus IX71 microscope equipped with a DP71 camera.

Morphological analysis. Cells were plated at 30–40% confluence and allowed to adhere overnight before treatment with adenovirus in serum-free media. After 48 h, cells were stimulated with 10 ng/ml PDGF or vehicle control for 30 min before imaging. Fluorescent cells were quantified using a custom-written MATLAB algorithm.

Adhesion assay. Cell adhesion was measured as described previously with minor modifications (43). A 96-well plate was coated with 10 μg/ml collagen I for 1 h, and nonspecific adhesion was blocked by 1-h incubation in 1% heat-denatured bovine serum albumin. Adenoviral-transduced cells were trypsinized, neutralized with trypsin-neutralizing solution, pelleted by centrifugation, resuspended to a final concentration of 1×10^5 cells/ml in serum-free media, and incubated at 37°C for 30 min. Cells were again centrifuged, resuspended in phosphate-buffered saline (PBS) containing divalents (0.9 mM $CaCl_2$ and 0.49 mM $MgCl_2$) as well as 2 mM dextrose (PBSD), and then seeded at 1×10^4 cells per well. After cells were allowed to adhere for 30 min, an initial fluorescence reading was taken at 485-nm excitation and 535-nm emission. Plates were then washed three times in PBSD before taking a final reading. Adherent fraction is defined as final fluorescence over initial fluorescence.

Collagen gel contraction. Type I rat tail collagen was diluted in 5× serum-free DMEM and then buffered to a final pH of 7.4 using sodium hydroxide and acetic acid. Cells transduced with either AdGFP or AdPoldip2 were suspended in serum-free DMEM and mixed with the collagen solution to create a final mixture of 1.5 mg/ml collagen. The solution was swirled to mix, and 400 μl containing a total of 2.5×10^5 cells was pipetted into a 24-well plate. Gels were polymerized at 37°C and then incubated in DMEM containing 10% fetal calf serum for 18 h to allow cells to spread. Finally, gels were detached and incubated with PDGF (10 ng/ml) for 24 h before imaging. Percent gel contraction was calculated as 100 × (initial gel area − final gel area)/initial gel area. All areas were quantified by tracing the contracted gels in ImageJ.

Focal adhesion turnover assay. Nocodazole-induced, microtubule-dependent focal adhesion turnover was carried out as described previously by others (15). VSMCs were plated and grown to 50–60% confluence before treatment with adenovirus or transient transfection with siRNA for 72 h. For some experiments, both treatments were given simultaneously. Three days after adenovirus treatment in serum-free DMEM, VSMCs were incubated with 10 μM nocodazole for 4 h to completely depolymerize microtubules. Nocodazole was washed out with serum-free DMEM to allow microtubule repolymerization, which leads to dissolution of existing focal adhesions followed by formation of new ones. Cells were fixed at the indicated time points in 4% formaldehyde in PBS for 10 min or in acetone:methanol (1:1) at −20°C for 20 min followed by permeabilization with 0.5% Triton-X 100 in PBS for 5 min, before the processing for immunofluorescence. In some experiments, protein was collected for Western blot studies.

Focal adhesion segmentation. Images of cells stained for either paxillin or FAKpY397 collected as previously described were quantified in a custom-written MATLAB routine. After background subtraction, Otsu's method was used to segment nuclei and focal adhesions in transduced cells. If cells were in contact, a seeded watershed algorithm was performed to determine the cell boundary. Overlapping focal adhesions were divided by a watershed filter after subtracting the low-pass filtered image from the original image. Focal adhesions that exceeded the average area within each cell by three standard deviations and also had low solidity were considered to be overlapping. The size of the low-pass filter was determined based on the average focal adhesion size within the cell. Over 1,000 focal adhesions per condition were quantified by the number per cell area as well as the average area of each these focal adhesions.

Measurement of reactive oxygen species production at sites of focal adhesions with FAT-HyPer. To measure intracellular reactive oxygen species (ROS) production, we used the genetically encoded specific H_2O_2 sensor HyPer (4). This fluorescent probe consists of the bacterial H_2O_2-sensitive transcription factor OxyR fused to circularly permuted yellow fluorescent protein, which produces two excitation peaks (420 nm and 500 nm) and single emission peak (516 nm). The ratio of fluorescence intensity following sequential excitation at each peak is sensitive to H_2O_2 concentration and is rapidly reversible, allowing live cell dynamic monitoring of intracellular H_2O_2 concentration (29).

To target the HyPer probe to focal adhesions, we used a focal adhesion targeting (FAT)-HyPer fusion protein generated by Dr. Terada. The FAT domain of human FAK (residues 896–1129) was recovered from a human umbilical vein endothelial cell library by PCR with the addition of a Kozak consensus. This FAT domain was used to replace the NH_2-terminal mitochondrial targeting sequence in pHyPer-dMito (Evrogen, Moscow, Russia) at Nhe I and Bam HI sites, downstream of a CMV promoter.

For experiments, VSMCs were seeded at 30–40% confluence in 35-mm collagen I-coated MatTek culture dishes and maintained in DMEM containing 10% FBS for 24 h before transfection. For transient transfections, the cells were rinsed with PBS and were transfected with FAT-HyPer ± Poldip2 (N-myc rat Poldip2 in pcDNA3.1+) plasmids using Attractene Transfection Reagent (Qiagen) according to the manufacturer's protocol. Six hours after transfection, the cells were washed once with PBS, and fresh serum-free DMEM was added to the cells. After a further 48 h of incubation, nocodazole-induced, microtubule-dependent focal adhesion turnover was carried out as described above. For the hour following nocodazole washout, cells were sequentially excited by 405- and 488-nm lasers at 7–10% laser power, and emission was detected every minute at 500–530 nm with a HyD sensor using a Leica TCS SP5 laser-scanning confocal microscope (Buffalo Grove, IL). To calculate HyPer ratio images, we utilized LAS-AF software (Leica Microsystems, Jena, Germany).

Quantification of HyPer images was carried out as above for focal adhesion segmentation with minor modifications. First, cell bodies were manually segmented by visual inspection. Focal adhesions were next segmented independently at each excitation wavelength and then combined to form a single binary image of segmented focal adhesions. The average HyPer ratio, as well as focal adhesion area, was then determined from the segmented focal adhesions within the cell body.

Immunoblotting. VSMCs were lysed in Hunter's buffer (25 mM HEPES, 150 mM NaCl, 1.5 mM $MgCl_2$, 1 mM EGTA, 10 mM Na-pyrophosphate, 10 mM NaF, 0.1 mM Na-orthovanadate, 1% Na deoxycholate, 1% Triton X-100, 0.1% SDS, 10% glycerol, and protease inhibitors), and whole cell lysates were utilized for Western blot as described previously (12, 18, 27). Proteins were separated using SDS-PAGE and transferred to nitrocellulose membranes, blocked, and incubated with appropriate primary antibodies. Proteins were detected by enhanced chemiluminescence (Amersham, Pittsburgh, PA). Band intensity was quantified by densitometry using ImageJ 1.38 software.

Immunocytochemistry and confocal microscopy. Immunocytochemistry was carried out as described previously (21, 27). VSMCs were plated on collagen-coated glass coverslips, transiently transfected with siRNA for 72 h, or grown to 50–60% confluence before treatment with adenovirus. After the treatment period, cells were fixed and incubated with primary antibodies for FAKpY397 (focal adhesions), HA-tagged-RhoA, tubulin, and DAPI (nuclei) for 1 h. Secondary antibodies conjugated to specific fluorophores were used for detection. Vectashield mounting medium (Vector Laboratories, Burlingame, CA) was used for confocal experiments. Images were acquired with a Zeiss LSM 510 META Laser Scanning Confocal Microscope System using a Plan-Apo ×63 oil objective lens (NA = 1.40) and Zeiss ZEN acquisition software. Controls with no primary antibody showed no fluorescence, and single-label controls were performed in all multiple-labeling experiments. When cells from different treatment groups were compared, all image threshold settings of the confocal microscope remained constant. Mean intensity fluorescence was measured using Image-Pro Plus v.6.2 by selecting at least four representative fields of identical settings.

Rho activity assay. Rho activity was measured using the G-LISA method per the manufacturer's instructions (Cytoskeleton, Denver, CO). Briefly, experiments were timed so that all cell lysates could be collected and assayed at the same time without a freeze/thaw, and the amount of active GTP-bound Rho was detected with a specific RhoA antibody and luminometry.

Preparation of polyacrylamide substrates. Preparation of polyacrylamide substrates was carried out using Pelham and Wang's (39) previously published protocol with minor modifications. Coverslips were sequentially flamed and incubated in 0.1 N NaOH, followed by silanization by incubation for 10 min in 1.0% (vol/vol) 3-aminopropyltrimethoxysilane (TCI America, Portland, OR). Residual silane was removed by extensive rinsing in distilled H_2O, and then coverslips were activated by 30-min incubation in 0.5% glutaraldehyde (Bio-Rad). Compliant gels consisting of 10% acrylamide and 0.13% bis-acrylamide embedded with 200-nm red fluorescent nanoparticles (Invitrogen) were then polymerized. To allow for cell adhesion, sulfo-SANPAH (Thermo Scientific, Waltham, MA) was used to covalently link collagen I (BD Biosciences) to the surface. Uniaxial compression testing was performed on a Bose EnduraTEC ELF 3200 Uniaxial Testing System to a maximum of 10% strain yielding a Young's Modulus of 20.4 ± 0.16 kPa.

Traction force microscopy. Cells were plated at 1,000 cells/cm^2 on collagen-coated polyacrylamide substrates including 200-nm fluorescent microbeads, allowed to adhere overnight, transduced the following day, and cultured for 3 days before the experiments were begun. Thirty minutes before the imaging, the cell culture medium was replaced with serum-free DMEM with or without PDGF. Traction force cytometry was then performed as described with a Nikon Eclipse Ti inverted epifluorescence microscope (Melville, NY) equipped with an environmental chamber (In Vivo Scientific, St. Louis, MO). An average of six cells per substrate was captured; values represent an average of three to seven experiments. Particle displacements were determined by comparison of stressed and unstressed gel images and used to determine traction forces with a Fourier-transform traction force cytometry (8) in a custom-written MATLAB routine. To calculate polarization, the magnitude of these traction forces was used to generate a force-weighted center of mass for each cell. The polarization was defined as the distance between force-weighted center of mass and the unweighted center of mass of the entire cell (30).

Statistical analysis. Results are expressed as mean ± SE. Statistical significance was assessed using either *t*-test or ANOVA, followed by contrast analysis. A value of $P < 0.05$ was considered significant.

RESULTS

Poldip2 overexpression inhibits VSMC migration. We previously showed using a Boyden chamber assay that manipulation of Poldip2 levels affects VSMC migration without examining in detail the effect of Poldip2 on the phenotype of the migrating cell (27). To visualize the phases of migration potentially affected by Poldip2, we performed a live-cell wound-healing assay. Consistent with our previous data, the PDGF (10 ng/ml)-stimulated wound-healing process is significantly reduced in AdPoldip2 cells (Fig. 1*A* and Supplemental Video S2; supplemental material for this article is available online at the *American Journal of Physiology Heart and Circulatory Physiology* website). Compared with AdGFP cells (Fig. 1*A* and Supplemental Video S1), cells transduced with

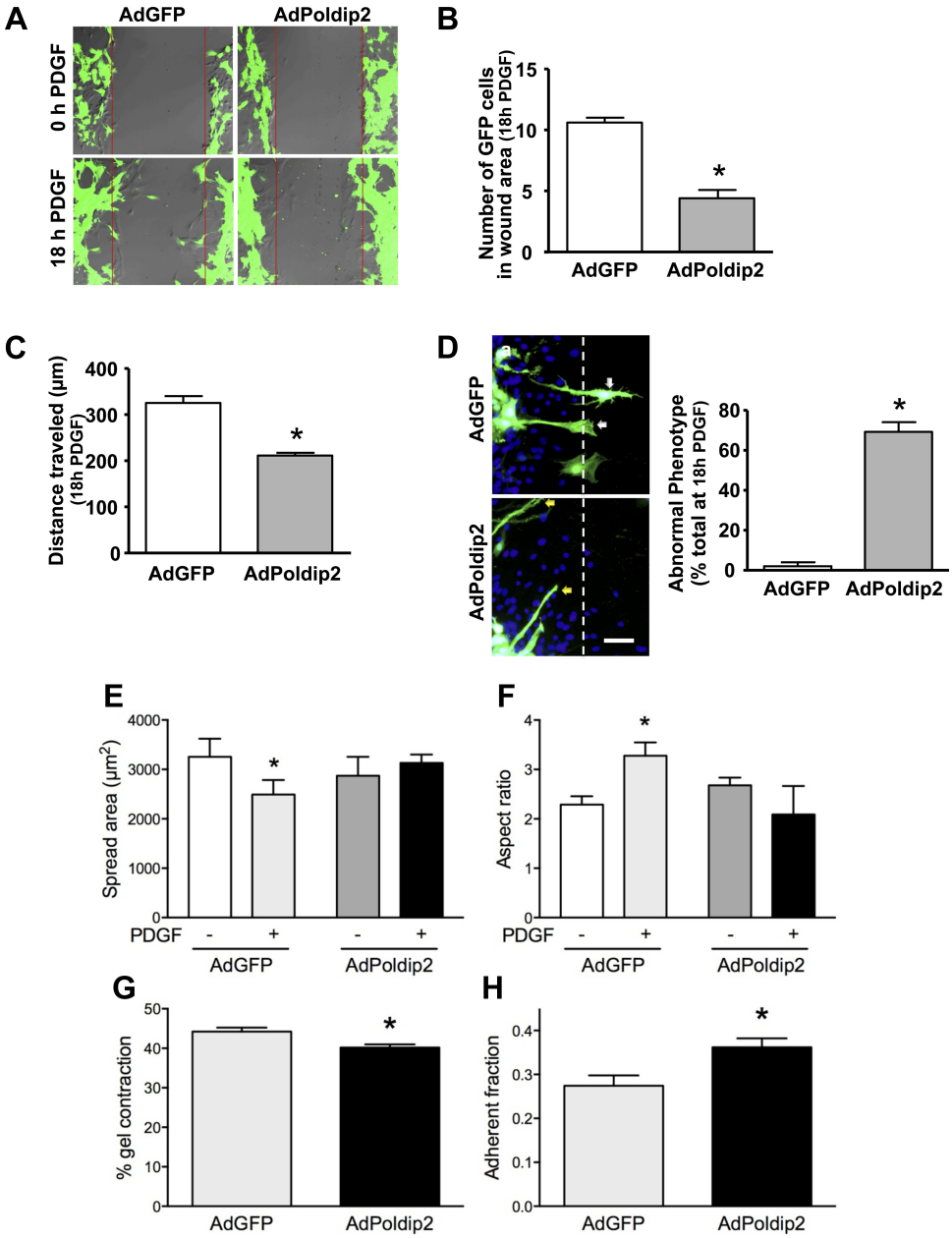

Fig. 1. Polymerase-δ-interacting protein 2 (Poldip2) overexpression inhibits vascular smooth muscle cell (VSMC) migration and contraction but increases adhesion. *A*: confluent VSMC layer was wounded and subjected to PDGF (10 ng/ml) stimulation for 18 h while cell migration was recorded using live-cell confocal microscopy. Images of green fluorescent protein-expressing adenovirus (AdGFP)- or AdPoldip2-transduced cells at 0 h or after 18 h with PDGF are representative of 3 independent studies. Quantitative analysis of the number of GFP-positive cells in the wound area (*B*) and total distance (μm) traveled (*C*) after 18 h of PDGF are shown. Bars for *B* and *C* are means ± SE of 5 independent fields, in which at least 5 cells were measured, $*P < 0.05$. *D*: confluent VSMC layer was wounded and subjected to PDGF (10 ng/ml) stimulation for 24 h. Cells with retracting tails are apparent after AdGFP transduction (white arrows). Long cytoplasmic extensions in AdPoldip2-transduced cells are also visible (yellow arrows). Green fluorescence indicates transduced cells. Nuclei are labeled with DAPI (blue). Images are representative of 3 studies. Bar graph summarizes the quantitative analysis of cells with long cytoplasmic extensions in the wound area, which represent an abnormal phenotype. Bars are mean ± SE of 5 independent fields, in which at least 5 cells were measured in 3 independent experiments, $*P < 0.05$. Scale bar = 100 μm. *E* and *F*: cells transduced with either AdGFP or AdPoldip2 were stimulated with either PDGF or vehicle control for 30 min, and area (*E*) and aspect ratio (*F*) were calculated as described. Bars represent mean ± SE of at least 3 independent experiments with over 50 cells per condition, $*P < 0.05$ relative to control. *G*: transduced cells were allowed to contract 1.5 mg/l collagen I gels for 24 h in the presence of 10 ng/ml PDGF. Values represent the average ± SE of 3 independent experiments with 4 wells per experiment. $*P < 0.05$. *H*: adherence of transduced cells was measured as described in MATERIALS AND METHODS. Values represent the average ± SE of 3 independent experiments with 4–8 wells per experiment. $*P < 0.05$.

AdPoldip2 show a significant reduction in the number of cells entering the wound area (Fig. 1*B*) as well as total distance traveled (Fig. 1*C*) into the wound area. In addition, we observed an abnormal phenotype in AdPoldip2 cells. PDGF-stimulated, AdGFP-transduced cells showed a polarized cell shape with clear translocation of the cell body into the wound-healing area with retracting tails (Fig. 1*D*). In contrast, AdPoldip2-transduced cells began to migrate by producing very long, unstable cytoplasmic extensions at the leading migratory front of the cell but were unable to translocate the cell body (Fig. 1*D* and Supplemental Video S2). This abnormal phenotype was present in ~70% of AdPoldip2-transduced cells in the wound area. Moreover, in AdGFP-treated cells, PDGF reduced cell spreading and increased the aspect ratio (major axis divided by the minor axis), whereas, in AdPoldip2-treated cells, PDGF had no effect on either parameter (Fig. 1, *E* and *F*). It should be noted that cytoplasmic extensions were not observed during short exposures to PDGF. Taken together, these data clearly demonstrate that overexpression of Poldip2 significantly reduces migration.

Poldip2 overexpression inhibits focal adhesion dissolution but not cell contraction. Our previous data demonstrating activation of RhoA upon Poldip2 overexpression suggest that migratory events downstream of RhoA might account for the abnormal phenotype shown in Fig. 1*D*. We therefore examined the effect of Poldip2 overexpression on cell body contraction, focal adhesion turnover, and polarization. Using a gel-contraction assay, we observed only a small decrease in cell contraction in response to PDGF in AdPoldip2-transduced cells compared with AdGFP-infected cells (Fig. 1*G*), suggesting that contraction is relatively normal in these cells and does not account for failure of the cell body to move. An effect of

Poldip2 on focal adhesion turnover is more likely, however, because we previously observed strong focal adhesions in Poldip2-overexpressing cells (12, 27). Indeed, incubation of cells with AdPoldip2 significantly increased adherence to substrate (Fig. 1*H*), suggesting that migration might be impaired by dysfunction of focal adhesion turnover. Whether this occurs through inhibition of focal adhesion dissolution or enhancement of focal adhesion formation is unclear. These potential mechanisms were investigated using a nocodazole-induced, microtubule-dependent focal adhesion turnover assay (15).

In this assay, nocodazole (10 μmol/l, 4 h) incubation depolymerizes microtubules (compare Fig. 2*A*, *a* and *c*). Removal of nocodazole initiates microtubule repolymerization between 5 and 15 min, which subsequently induces dissolution of focal adhesions with a peak effect at 30 min, as indicated by a significant reduction in the focal adhesion marker paxillin (Fig. 2*A*, *m*) and FAK phosphorylation on Y397 (FAKpY397) (Fig. 2*B*, *u*). By 60 min, reformation of microtubules (Fig. 2*A*, *g* and *h*) induces creation of new focal adhesions (Fig. 2*A*, *o*, and Fig. 2*B*, *w*). Thus this assay allows detection of both the dissolution

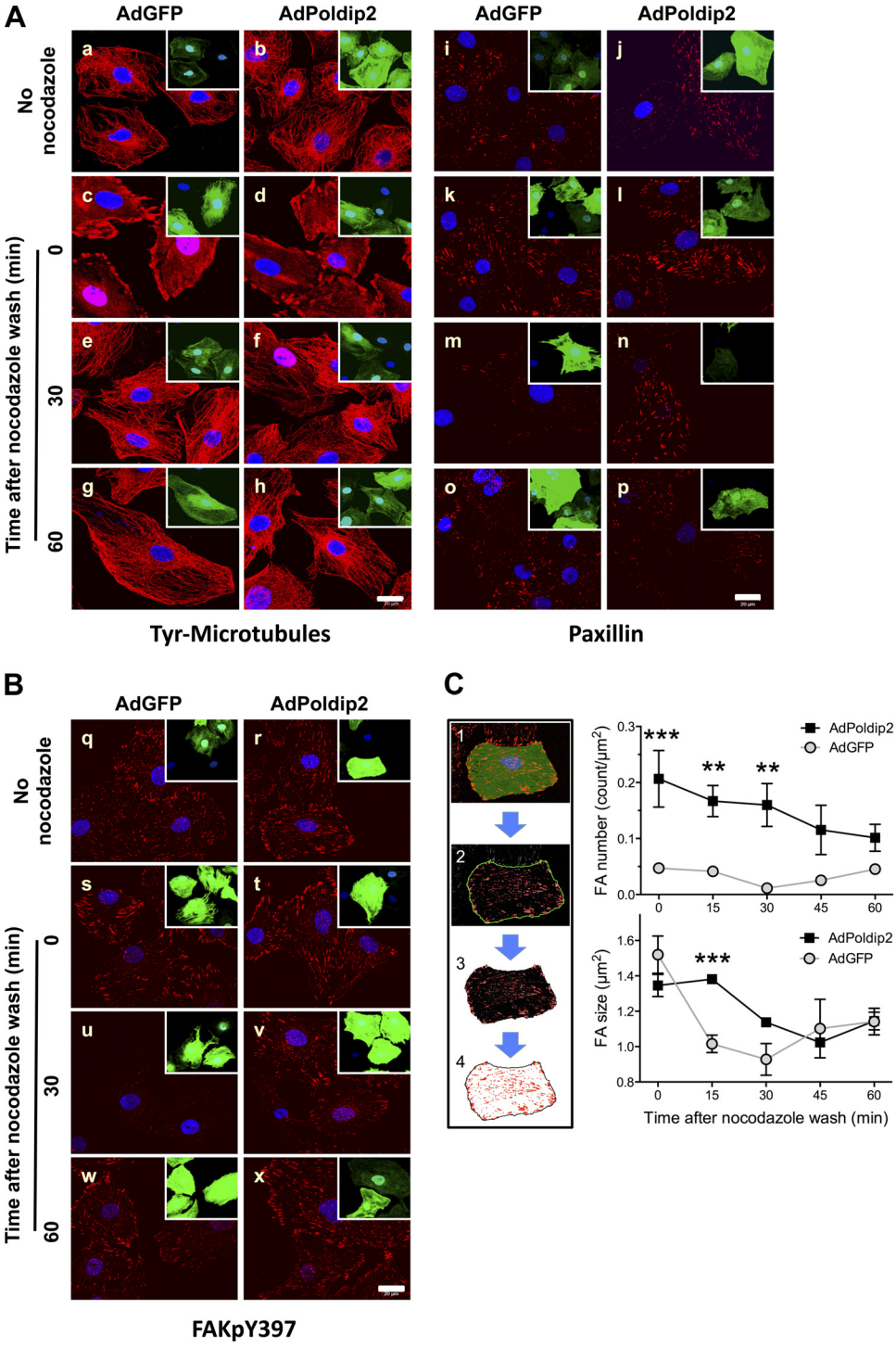

Fig. 2. Poldip2 overexpression inhibits nocodazole-induced, microtubule-dependent focal adhesion turnover, but not microtubule depolymerization. VSMCs were transduced with either AdGFP or AdPoldip2 for 72 h in serum-free DMEM before incubation with or without nocodazole (10 μmol/l) for 4 h. Cells were washed with fresh serum-free DMEM, fixed at the indicated time points, and immunostained for tyrosinated microtubules (Tyr-Microtubules) (*A*, *left*), paxillin (*A*, *right*), or FAKpY397 (*B*) (all are in red). Green color is an indication of control (AdGFP) or Poldip2 (AdPoldip2)-overexpressing cells (inset at the top right corner of each image). Nuclei are labeled with DAPI (blue). Images are representative of 3 experiments. *C*, *left*: sequential segmentation algorithm used to isolate focal adhesions (FA). *Right*: quantification of FAKpY397 staining in *B* with respect to number of focal adhesions per square micron (*top*) and average focal adhesion size (*bottom*). At least 1,000 focal adhesions were measured per condition. Data include 15- and 45-min time points that were omitted from previous panels for clarity and represent average ± SE. $^{**}P < 0.01$, $^{***}P < 0.001$ relative to the other treatment condition.

and formation of focal adhesions. Poldip2-overexpressing cells maintained focal adhesions after nocodazole washout (Fig. 2*A*, *n*, and Fig. 2*B*, *v*), indicating that Poldip2 overexpression prevents focal adhesion dissolution. We quantified these changes by segmenting individual focal adhesions over a more complete time course (Fig. 2*C*, *left*). AdPoldip2 cells had significantly more focal adhesions immediately after washout, and this increase was maintained through 30 min (Fig. 2*C*, *top*, *right*). The decrease in focal adhesion area after nocodazole washout in AdGFP cells was significantly delayed in AdPoldip2 cells (Fig. 2*C*, *bottom*, *right*). Thus dissolution of established focal adhesions in response to nocodazole washout at 15 min is unable to occur in AdPoldip2 cells.

Poldip2 overexpression inhibits dynamic changes in local H_2O_2 levels during focal adhesion turnover. Multiple previous studies have shown that changes in the intracellular ROS concentration can severely affect the fate of focal adhesions (10, 16, 17, 25, 37). ROS scavengers such as *N*-acetyl cysteine and flavin oxidase inhibitors such as diphenyleneiodonium can cause dissolution of focal adhesions, whereas intracellular increases in H_2O_2 can activate FAK and consequently stimulate cell adhesion and spreading. To investigate Poldip2-dependent changes in local H_2O_2 concentrations in focal adhesions, we used cells transfected with focal adhesion-targeted FAT-HyPer during the nocodazole assay. Ratiometric analysis of acquired images (Fig. 3) revealed that the initially high level of H_2O_2 localized to focal adhesions decreased (color change from pink to blue) concurrently with dissolution of focal adhesions, with lowest H_2O_2 levels detected at $<$15 min after nocodazole washout. This change in local H_2O_2 levels is followed by dissolution of focal adhesions. Over the next 30 min, H_2O_2 levels slowly increase at the sites of newly formed focal contacts/adhesions (Fig. 3*A*, *bottom*, arrows). In Poldip2-overexpressing cells, this decrease in H_2O_2 levels after nocodazole washout was abolished (Fig. 3*A*, *top*, arrows), which parallels the persistence of focal adhesions in these cells. This interpretation is confirmed by the time course of HyPer signal calculated from focal adhesions, where H_2O_2 concentration was markedly decreased between 0 and 60 min in control cells but was sustained and even increased in cells transduced with AdPoldip2 (Fig. 3*B*).

Poldip2-induced focal adhesion stabilization is RhoA dependent. As described above, we previously showed that Poldip2 overexpression increases RhoA activity in VSMCs (27). To determine whether RhoA mediates the Poldip2-induced focal adhesion stabilization observed in Fig. 2, we first examined RhoA activity during dynamic focal adhesion turnover after nocodazole washout. RhoA activity was similar in AdGFP and AdPoldip2 cells immediately after washout, perhaps attributable to the stimulatory effect of microtubule depolymerization on Rho activity (46), but was clearly higher in AdPoldip2 cells at 30 min after nocodazole washout (Fig. 4*A*), indicating a possible role of RhoA in Poldip2-induced focal adhesion stabilization. To determine whether the ability to maintain RhoA in an active state is responsible for the effects of Poldip2 on focal adhesion turnover, we used the cell-permeable Rho inhibitor C3 transferase (2 μg/ml, 4 h) in the nocodazole assay. C3-transferase had no effect on focal adhesions in AdPoldip2-treated cells at 0 min after the wash (Fig. 4*C*), but, at 30 min after the wash, Rho inhibition significantly blocked the ability of Poldip2 to prevent focal adhesion dissolution (Fig. 4, *B* and *D*).

Endogenous Poldip2 mediates focal adhesion formation via FAK, RhoA, and Nox4. To determine whether endogenous Poldip2 normally regulates focal adhesion turnover, we used siRNA-mediated reduction of Poldip2. We have previously observed that knockdown of Poldip2 results in decreased staining for the focal adhesion markers paxillin and vinculin (27). Indeed, as shown in Fig. 5, knockdown of Poldip2 results in a phenotype of reduced focal adhesions, as measured by dephosphorylation of FAK on Y397 by Western blot or immunocytochemistry. We attempted to use the nocodazole assay to confirm an obligatory role of Poldip2 in focal adhesion turnover. However, these cells lack detectable focal adhesions before nocodazole treatment, and there are no new focal adhesions formed up to 2 h after the wash (data not shown). From this we concluded that lack of Poldip2 also prevents focal adhesion formation in VSMCs, a process also reliant on Rho family GTPases (45). In support of this observation, the siPoldip2 focal adhesion phenotype is completely rescued by overexpression of constitutively active RhoA or wild-type FAK (Fig. 5*B*).

We have previously shown that Poldip2 interacts with Nox4 and positively regulates its function (27). However, it is not clear how much of the Poldip2 effect is Nox4 dependent. Similar to siPoldip2, siNox4 reduces FAKpY397 phosphorylation (Fig. 6*A*), and its effects on focal adhesions can be rescued by overexpression of constitutively active RhoA (Fig. 6*B*). To determine whether Poldip2 requires Nox4 to regulate focal adhesions, we used overexpression and knockdown strategies in combination. The ability of Poldip2 to enhance focal adhesion formation and induce FAKpY397 phosphorylation is completely lost when cells are cotreated with siNox4 (Fig. 7, *A–C*). Taken together, these experiments clearly show that Nox4 is required for stabilization of focal adhesions by Poldip2, most likely by activating RhoA/FAK.

Poldip2 regulates traction forces and polarization in PDGF-treated VSMCs. The force exerted on the substrate is a direct consequence of focal adhesion engagement and intracellular contraction. In migratory cells, the dynamic turnover of focal adhesions leads to the reorientation of traction forces. Polarization of traction forces is necessary for appropriate cell body contraction, as either excess or inadequate traction forces inhibit retrograde actin flow (an indicator of myosin-dependent contraction forces) in slow-moving cells (22). Because Poldip2 overexpression decreases focal adhesion turnover (Fig. 2), we hypothesized that it would also affect traction forces and cell polarization. Using traction force microscopy, we investigated VSMCs in basal and PDGF-stimulated conditions (Fig. 8*A*). Poldip2-overexpressing cells had similar traction forces compared with control cells in unstimulated conditions, consistent with the absence of effect of Poldip2 on contraction. PDGF treatment caused a significant decrease in the traction forces in control AdGFP cells, indicating dynamic changes in focal adhesions. In contrast, the traction forces remained unchanged after PDGF stimulation in AdPoldip2 cells (Fig. 8*B*). In parallel to decreased traction forces, AdGFP cells showed a significant increase in traction force polarization, which is measured as the distance between the traction force-weighted center of mass and the geometric center of the cell, whereas AdPoldip2 cells failed to polarize (Fig. 8*C*). This suggests that

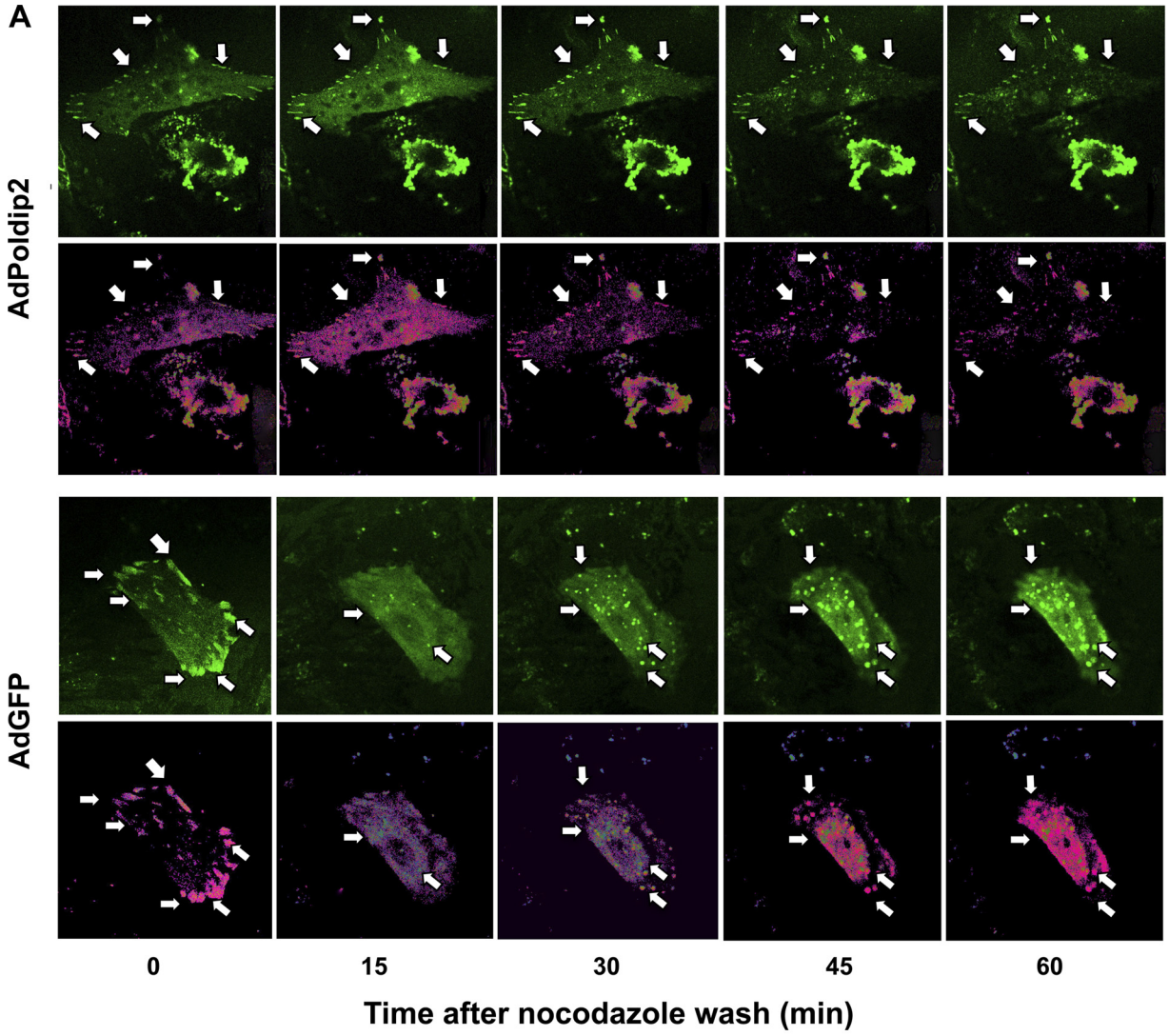

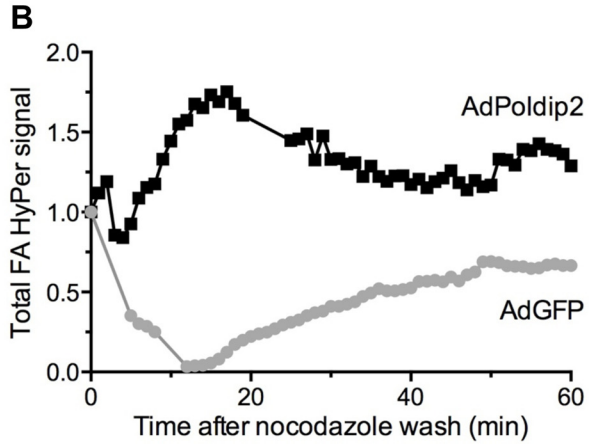

Fig. 3. Poldip2 overexpression prevents dynamic changes in local H_2O_2 levels in focal adhesions during nocodazole-induced focal adhesion turnover. VSMCs transiently transduced with focal adhesion-targeted (FAT)-HyPer and AdGFP or AdPoldip2 were serum starved for 24 h before nocodazole (10 μmol/l, 4 h) treatment. After nocodazole washout, relative H_2O_2 concentration at sites of focal adhesions was assessed at indicated times based on ratiometric analysis of the FAT-HyPer signal. Shown are images from 1 experiment repeated twice. *A*: time-dependent change in intensity and distribution of FAT-HyPer signal in AdPoldip2-transduced cells (*top*) or control cells (*bottom*). Arrows indicate sites of focal adhesions. *Top*: FAT-HyPer signal. *Bottom*: ratiometric analysis of FAT-HyPer 488/405 excitation signals. Change of color from blue to pink indicates an increase in relative H_2O_2 concentration. *B*: time course of H_2O_2 in a single cell normalized to *time 0* after nocodazole wash based on ratiometric analysis of FAT-HyPer 488/405 excitation signals and focal adhesion segmentation.

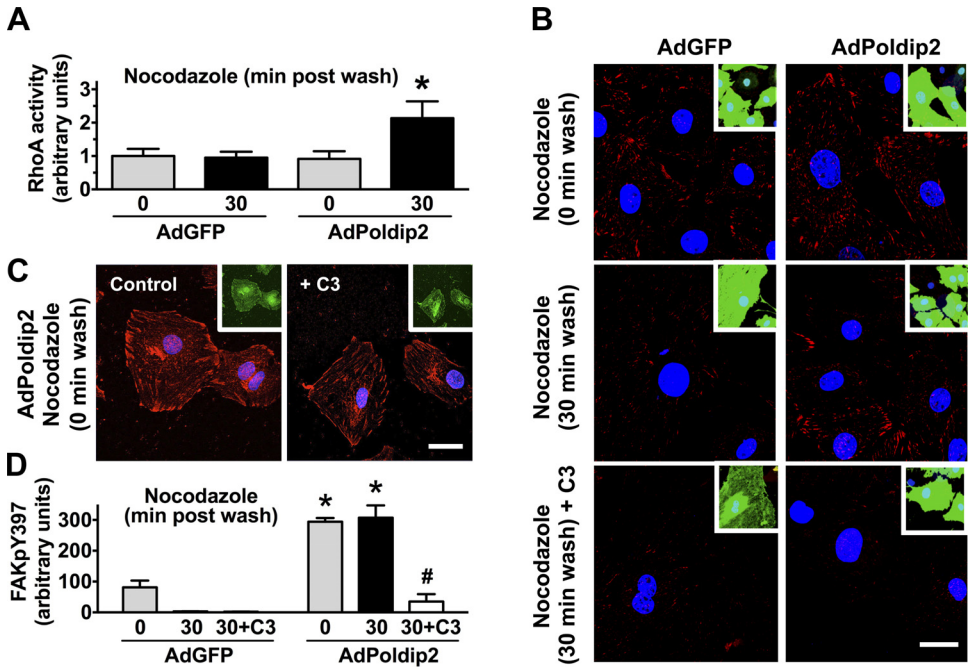

Fig. 4. Overexpression of Poldip2 induces focal adhesion stabilization via RhoA. *A*: RhoA activity, as measured using the G-LISA method, in control (AdGFP) or Poldip2-overexpressing cells (AdPoldip2) subjected to the nocodazole-induced focal adhesion turnover assay. Data represent means ± SE of 4 independent experiments. *$P < 0.05$ vs. AdGFP at 30 min. *B–D*: VSMCs transduced with AdGFP or AdPoldip2 were incubated with nocodazole (10 μmol/l, 4 h) in the presence or absence of the Rho inhibitor C3 transferase (2 μg/ml). At *time 0* (*C*) or 30 min after nocodazole washout (*B*), cells were immunostained for focal adhesion kinase (FAK)pY397 (red). Nuclei are labeled with DAPI (blue). Green color (*inset*) is an indication of the control (AdGFP) or Poldip2 (AdPoldip2)-overexpressing cells. Pictures are representative of 3 experiments. C3 transferase was maintained throughout the experimental period. Scale bar = 20 μm. *D*: quantification of FAKpY397 immunofluorescence. Bars represent means ± SE of 3–4 independent experiments. *$P < 0.05$ vs. AdGFP, #$P < 0.05$ vs. AdPoldip2 without C3.

the defect in focal adhesion turnover in Poldip2-overexpressing cells contributes to failure of traction force polarization, which blocks migration.

DISCUSSION

This study was designed to probe the molecular mechanism by which Poldip2/Nox4 regulates VSMC migration. Migration is a complex process that is centrally dependent on Rho, and, starting from our previous observation that Poldip2 overexpression leads to an elevation of Rho activity (27), we tested several downstream effects of Rho to determine at which point in the migratory cycle Poldip2 regulation of Rho activity has a functional consequence. We found that Poldip2 controls both the formation and dissolution of focal adhesions. Its perturbation leads to failure of traction force polarization and thereby loss of the migratory phenotype. The failure of the cell body to move forward in Poldip2-overexpressing cells does not appear to be attributable to an inability of the cell to contract but rather to this initial failure of the cell to polarize, suggesting that the primary role of Poldip2 is to control focal adhesion dissolution (Fig. 9). Our results explain our previous observation that both knockdown and overexpression of Poldip2 prevent PDGF-induced migration of VSMCs (27) and identify RhoA/FAK as downstream targets of Poldip2. We also identify a possible role of Nox4 in Poldip2-induced focal adhesion stability. Taken together, our results unveil new mechanisms by which NADPH oxidases regulate Rho-dependent migratory processes that are critical events in occlusive vasculopathies.

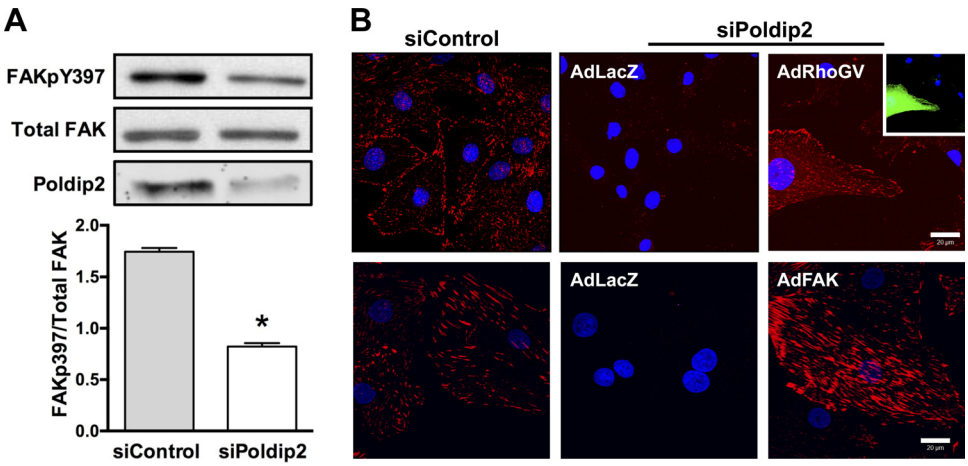

Fig. 5. Destabilization of focal adhesions by Poldip2 downregulation is rescued by RhoA or FAK. VSMCs were transiently transfected with control siRNA (siControl) or siPoldip2. *A*, *top*: protein was harvested after 72 h and immunoblotted with anti-FAKpY397, anti-FAK (total), and anti-Poldip2. *Bottom*: quantification of Western blots. Bars represent means ± SE of FAKpY397/total FAK in 7–9 independent experiments, *$P < 0.05$. *B*: following transfection with siRNA, VSMCs were transduced with control adenovirus (AdLacZ), constitutively active Rho (AdRhoGV), or FAK adenovirus (AdFAK). Cells were double-labeled with anti-FAKpY397 (red) to detect focal adhesions and anti-HA tag (green) to detect constitutively active RhoA. Nuclei are labeled with DAPI (blue). Images are representative of 3 experiments. Scale bar = 20 μm.

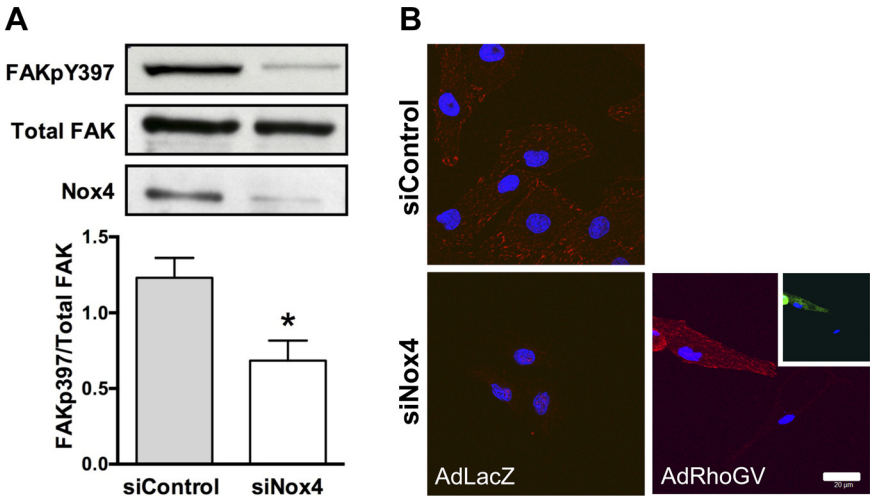

Fig. 6. Downregulation of NADPH oxidase 4 (Nox4) inhibits FAK phosphorylation, and focal adhesion disappearance is rescued by active RhoA. VSMCs were transiently transfected with control siRNA (siControl) or siNox4. *A*, *top*: protein was harvested after 72 h and immunoblotted with anti-FAKpY397, anti-FAK (total), and anti-Nox4. *Bottom*: quantification of Western blots. Bars represent means ± SE of FAKpY397/total FAK in 7–9 independent experiments, $*P < 0.05$. *B*: VSMCs were transiently transfected with siControl or siNox4 before transduction with control adenovirus (AdLacZ) or constitutively active Rho adenovirus (AdRhoGV). Cells were labeled with anti-FAKpY397 (red) to detect focal adhesions. Nuclei are labeled with DAPI (blue). Pictures are representative of 3 experiments. Scale bar = 20 μm.

Migratory cells require cytoskeletal reorganization to facilitate their forward movement. This involves the formation of new focal adhesions at the front and dissolution of established ones at the rear of migratory cells. The resulting cytoskeletal reorganization polarizes the cell, which leads to cytoskeletal-dependent contraction and force generation for forward movement. In the live-cell wound-healing assay, Poldip2-overexpressing cells display reduced migration after PDGF stimulation compared with control cells. As expected, control cells exhibit a polarized phenotype of extended lamellipodia at the front of the cell and retracting tails at the rear end (Fig. 1*D*), as well as an increased aspect ratio. These cells are thus capable of morphological changes, such as whole-cell elongation in response to PDGF. In contrast, Poldip2-overexpressing cells failed to acquire this migratory phenotype; instead, they form long unstable cytoplasmic extensions and seem to be unable to move their cell body (Fig. 1*D*), exhibiting no overall change in aspect ratio. As a result, there is a significant reduction in the number of cells entering, and total distance traveled into, the wound area in Poldip2-overexpressing cells (Fig. 1, *B* and *C*).

One possible explanation for the failure to adopt a migratory phenotype is that the Poldip2 overexpression might switch the cells to a more differentiated state. Indeed, we have previously shown that Nox4 is required for maintenance of differentiation (12). However, we see no difference in expression of the differentiation markers smooth muscle α-actin or calponin (unpublished observations) between AdGFP- and AdPoldip2-infected cells, suggesting that Poldip2/Nox4 is not sufficient to induce differentiation in these cells.

Therefore, on the basis of the collective observations that Poldip2-overexpressing cells fail to attain the migratory phenotype but do not assume a differentiated one, that the ability of these cells to contract is not substantively impaired, and our previous work showing strong focal adhesions in these cells, we investigated in depth the hypothesis that Poldip2 controls focal adhesion turnover. Because focal adhesions are constantly turned over during migration, formation of new focal adhesions or dissolution of established focal adhesions could be affected. Discriminating between these possibilities is difficult in migrating cells because of the temporal coexistence of both newly forming and dissolving focal adhesions. However, Ezratty et al. (15) recently reported a nocodazole-treated, microtubule-induced focal adhesion turnover model system, which allows one to study focal adhesion turnover in a synchronized fashion. We adapted this model for VSMCs and studied the role of Poldip2 in VSMC focal adhesion formation and dissolution. Of importance, in this assay, nocodazole-induced microtubule depolymerization and postwash-induced repolymerization processes are intact in Poldip2-overexpressing cells (Fig. 2*A*). However, in control cells, 30 min after nocodazole washout both functional (FAKpY397) (Fig. 2*B*) and structural (paxillin) (Fig. 2*A*) markers of focal adhesions are significantly decreased, indicating focal adhesion dissolution, whereas, in Poldip2-overexpressing cells, FAKpY397 (Fig. 2*B*) and paxillin (Fig. 2*A*) fluorescence signals remain strong. This suggests that focal adhesion dissolution is prevented, which potentially explains why PDGF stimulation failed to produce a polarized phenotype in these cells, instead forming abnormal long cytoplasmic extensions. The persistence of this phenotype also indicates that the effects of Poldip2 do not simply delay turnover of focal adhesions but rather increase their stability, thereby preventing the migration. The mechanism underling this process needs further investigation.

Morphological polarization is a necessary first step in migration, which involves multiple mechanisms that induce lamellipodial formation at the leading edge of the cell (24). However, formation of nascent focal adhesions is necessary for the stabilization of lamellipodia by anchoring them to the ECM (24). In AdPoldip2 cells, we noticed abnormal cytoplasmic extensions (Fig. 1*D*) but a failure to establish a normal polarized cell shape. These extensions indicate that actin polymerization takes place in these cells, and, because we found that the ability of cells to contract is not impaired by Poldip2 overexpression, it is likely that the strength and orientation of focal adhesions are responsible for this abnormal phenotype. Indeed, the inhibition of focal adhesion turnover in Poldip2-overexpressing cells likely leads to failure of focal adhesions to release, so that actin protrusion must occur while central focal adhesions are firmly anchored, leading to a narrow cytoplasmic protrusion rather than a true lamellipodium. Similarly, in si-Poldip2-treated cells, focal adhesion formation is impaired, leading to the same ultimate inability to properly anchor and migrate.

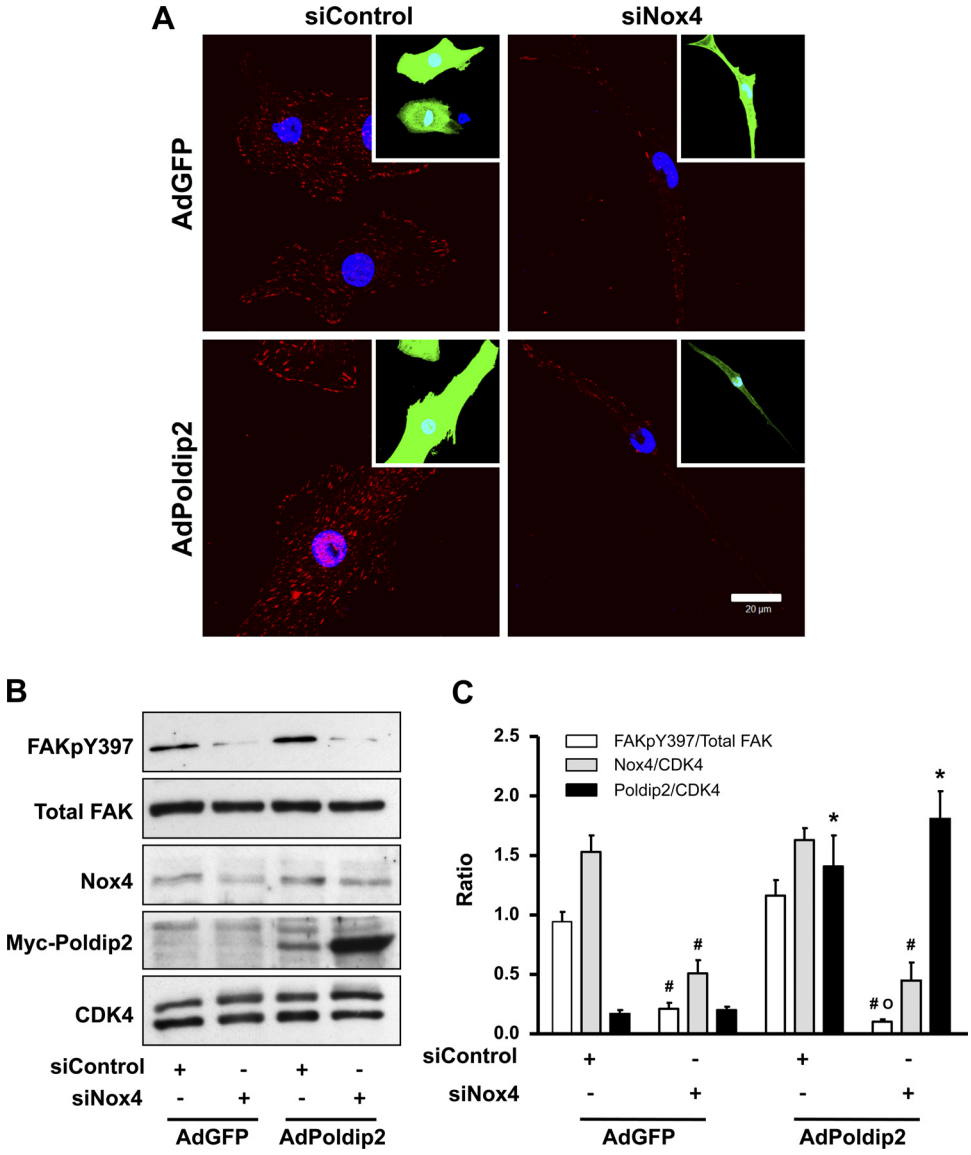

Fig. 7. Nox4 is required for Poldip2-induced focal adhesion stabilization. VSMCs were transiently transfected with siControl or siNox4. 2 days after transfection, cells were transduced with either control (AdGFP) or Poldip2 adenovirus (AdPoldip2) for 3 more days and fixed for either immunocytochemistry or immunoblotting. *A*: cells plated on coverslips were labeled with anti-FAKpY397 (red) to detect focal adhesions. *Insets*: green cells represent transduced cells. Nuclei are labeled with DAPI (blue). Scale bar = 20 μm. *B*: representative Western analysis for FAKpY397, FAK (total), Nox4, myc-Poldip2, and CDK4 (loading control). *C*: quantitative analysis of 3 independent Western experiments. Bars are means ± SE; #$P < 0.05$ vs. siControl; *$P < 0.05$ vs. AdGFP; °, not different from AdGFP with siNox4.

It has been observed that traction forces must be neither too great nor too weak to support contraction (22) and that they strongly influence cell shape, speed, and mode of movement. Traction forces thus need to be dynamic to facilitate migration. We found that PDGF stimulation decreases traction forces in control cells, consistent with the dynamic nature of focal adhesion turnover, and establishes an asymmetrical distribution of intracellular forces. However, in the Poldip2-overexpressing cells, PDGF stimulation neither decreases the traction forces nor establishes polarization of traction forces (Fig. 8*B*). This indicates that, in Poldip2-overexpressing cells, focal adhesions maintain static attachments and prevent the necessary PDGF-induced dynamic changes of the traction forces. Of interest, despite increased activity of both FAK and RhoA, which have been associated with increased traction forces (42), we did not observe any difference in basal traction forces upon Poldip2 overexpression. It has been reported that, once focal adhesions become mature by recruiting proteins such as zyxin, they lose the ability to generate traction forces and become passive anchorage devices (6). It is thus likely that the focal adhesions seen in Poldip2-overexpressing cells are mature and passive. Because the spatial and temporal patterns of traction forces have been reported to dictate cell body contraction and the direction of cell migration (22, 34), these observations may explain the reduced migration observed upon dysregulation of Poldip2.

It has previously been shown that Rho GTPases are major regulators of focal adhesion turnover and cytoskeletal reorganization. In migratory cells, regional alteration of Rac and RhoA activity facilitates cytoskeletal restructuring (36). We found no effect of Poldip2 overexpression on Rac activity (unpublished observations). This is functionally evident by the long cytoplasmic extensions noticed in the wound-healing assay in Poldip2-overexpressing cells (Fig. 1*D*). Moreover, the ability of the cells to contract was only slightly impaired by Poldip2 overexpression, suggesting that the elevation in RhoA that we previously reported (27) most likely affects focal adhesion turnover. Our data suggest that Poldip2/Nox4-dependent RhoA signaling is required for focal adhesion maturation and prevents dissolution, whereas lack of Poldip2 prevents the

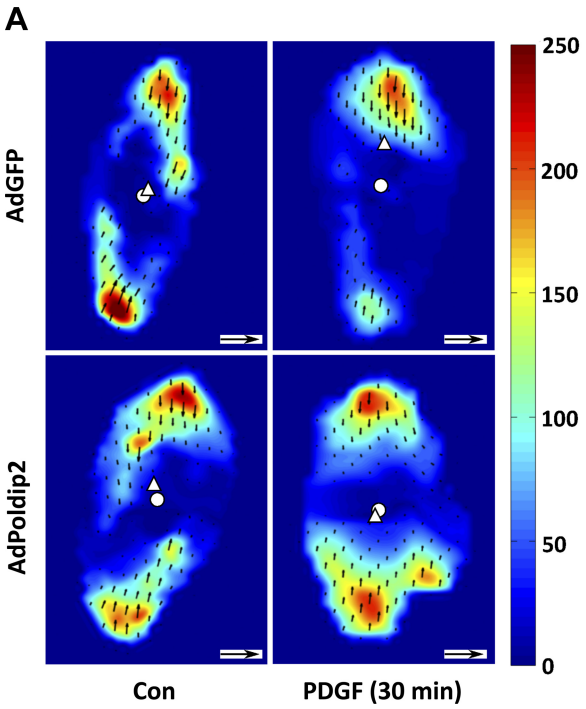

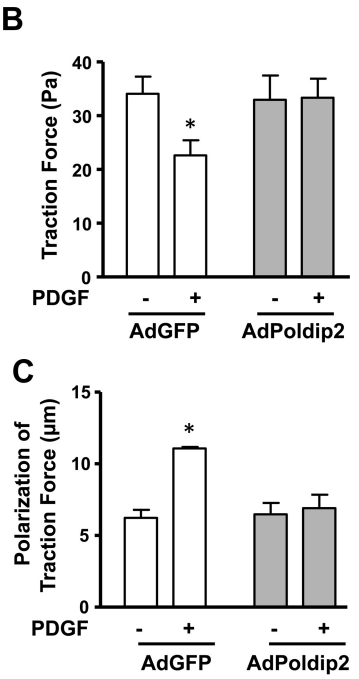

Fig. 8. PDGF-induced traction force reduction and polarization are attenuated in Ad-Poldip2 cells. Cells plated on a collagen matrix over a polyacrylamide layer including fluorescent microbeads were transduced with either AdGFP or AdPoldip2 for 72 h in serum-free DMEM before incubation with media or PDGF (10 ng/ml) for 30 min. Images of the cells and stressed gels were obtained before and 30 min after PDGF addition. An unstressed gel image was also taken after cell detachment with 2.5% trypsin. *A*: heat maps of traction stress magnitudes with the corresponding scale in Pascals. The white disc and triangle indicate the centers of the cell and of traction stresses, respectively. The small black arrows represent displacement vectors. Scale bar = 10 μm for cell size, inset scale arrow = 1.0 μm for displacement vectors. Bar graphs represent means ± SE of 3 or more independent experiments, each including measurements from 18–45 cells for median cell traction stresses (*B*) and polarization (*C*) in AdGFP and AdPoldip2 cells with and without PDGF stimulation. $^*P < 0.05$ vs. no PDGF.

formation of stable focal adhesions. Thirty minutes after nocodazole washout, when focal adhesion dissolution is at its peak in AdGFP cells, RhoA activity is significantly elevated in AdPoldip2-treated cells, and the number of focal adhesions remains elevated. Inhibition of Rho with C3 transferase completely reverses the Poldip2-induced inhibitory effect on focal adhesion dissolution (Fig. 4). These data strongly suggest that the major Rho-dependent effect of Poldip2 is on focal adhesion dissolution.

One of the effectors of RhoA is FAK, the phosphorylation of which plays a critical role in focal adhesion dynamics. In this study, Poldip2 downregulation significantly decreases FAK phosphorylation at Y397 (Fig. 5*A*), and this is prevented by overexpression of constitutively active RhoA or FAK (Fig. 5*B*). In some studies, RhoA is reported to be upstream of FAK activation and to induce focal adhesion (3, 14, 20, 23, 48). There is also evidence suggesting that FAK could activate RhoA via Rho guanine nucleotide exchange factor (RhoGEF) (11, 51). These disparate observations suggest a possible regulatory circuit between RhoA and FAK activation. Our observations suggest that ROS produced from Nox4/Poldip2 may control this pathway (Fig. 9). In support of this possibility, we observed high levels of H_2O_2 in the stable focal adhesions seen in Poldip2-overexpressing cells (Fig. 3) and a decrease in H_2O_2 as focal adhesions dissolve in control cells. Interestingly, a further increase in H_2O_2 levels in the focal adhesions of Poldip2-overexpressing cells following nocodazole washout occurs concomitantly with an increase in Rho activity. H_2O_2 has been previously shown to activate focal adhesion proteins by increasing their tyrosine phosphorylation (5, 17, 49), which plays an important role in focal adhesion maturation and turnover. Moreover, ROS have been shown to potentially activate RhoA via direct oxidative modification, although this conclusion is based on mutation studies rather than direct demonstration of oxidation (1, 27). We show here that H_2O_2 generation occurs in the same intracellular compartment as FAK, and, given the localization of Nox4, p22phox, and Poldip2 in VSMCs to focal adhesions (21, 27), our observations provide a framework to understand targeted, specific H_2O_2-dependent regulation of focal adhesion turnover. Exactly how RhoA and FAK are activated by ROS is unclear, but the mechanism could involve inactivation of the focal adhesion phosphatase PTP-PEST (32), the direct oxidation of Rho (1) or targeting of RhoGEF or RhoGAP.

Although Poldip2 has been shown to be a positive regulator of Nox4, it is not clear which functions of Poldip2 are mediated

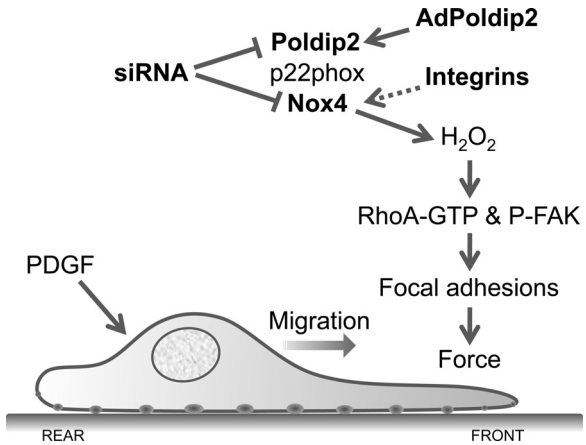

Fig. 9. Proposed model of control of VSMC migration by Poldip2. When PDGF initiates migration, H_2O_2 generated from the integrin-stimulated Nox4/Poldip2 complex can activate RhoA and increase FAK phosphorylation at tyrosine 397, leading to focal adhesion formation and generation of traction forces. Overexpression of Poldip2 leads to continuous H_2O_2 production and prevents dissolution of focal adhesions at the rear of the cell, causing long cytoplasmic extensions but inability to migrate and failure to polarize. Loss of Poldip2 or Nox4 leads to a reduction in FAKpY397 and a failure to form new focal adhesions.

by Nox4 because Poldip2 has been reported to have Nox4-independent effects as well (none so far on the cytoskeleton) (7). In the present study, both Poldip2 and Nox4 downregulation showed a similar phenotype, confirming our previous observations (27). The observation that Nox4 downregulation significantly inhibited FAK phosphorylation in the presence and absence of Poldip2 overexpression (Fig. 7) clearly suggests that Nox4 is required for Poldip2-induced focal adhesion stabilization. Taken together, our results support the possibility that the Nox4/Poldip2 complex plays an important role in focal adhesion turnover. However, to understand the Nox role in focal adhesion turnover, it is necessary to further study the direct role of ROS on these dynamic changes and, in particular, how subcellular compartmentalization affects ROS-dependent functions. Migration of vascular cells is strongly implicated in different diseases, including cancer angiogenesis, atherosclerosis, and restenosis. Nox4 has been reported to participate in the migration of endothelial cells (13), VSMCs (27, 31), and myofibroblasts (19). In this study, we provide insight into the mechanism by which Poldip2 and Nox4 regulate VSMC migration. Taken together, our data indicate that the Poldip2/Nox4 complex plays a major role in migration of VSMCs by controlling the focal adhesion turnover and cell body polarization in a RhoA/FAK-dependent manner. These observations point to potential therapeutic targets for the control of pathological migration of VSMCs.

ACKNOWLEDGMENTS

We thank Dr. J. David Lambeth for providing Nox4 antibody, Dr. Aviv Hassid for providing the LacZ and RhoGV adenoviruses, and Dr. Joseph C. Loftus for his gift of FAK adenovirus. Confocal microscopy data for this study were acquired in the Microscopy in Medicine Core (MiM Core) at Emory University.

GRANTS

This work was supported by NIH grants HL38206, HL092120, and HL058863, as well as the National Science Foundation (1032527) and the Emory/Georgia Tech Regenerative Engineering and Medicine Center.

DISCLOSURES

No conflicts of interest, financial or otherwise, are declared by the authors.

AUTHOR CONTRIBUTIONS

Author contributions: S.R.D., D.J.M., S.V., L.P.H., L.P., M.L., B.S.-R., and M.K.K. performed experiments; S.R.D., D.J.M., S.V., and B.L. analyzed data; S.R.D., D.J.M., S.V., and B.L. prepared figures; S.R.D. drafted manuscript; S.R.D., D.J.M., S.V., L.P.H., A.N.L., L.P., M.L., B.S.-R., L.L.H., L.S.T., M.R.D., B.L., and K.K.G. approved final version of manuscript; S.V., L.P.H., L.L.H., L.S.T., M.R.D., and K.K.G. interpreted results of experiments; L.P.H., A.N.L., L.L.H., L.S.T., M.R.D., B.L., and K.K.G. edited and revised manuscript; A.N.L., L.L.H., B.L., and K.K.G. conception and design of research.

REFERENCES

1. **Aghajanian A, Wittchen E, Campbell S, Burridge K.** Direct activation of RhoA by reactive oxygen species requires a redox-sensitive motif. *PLoS One* 4: e8045, 2009.
2. **Akagi T, Murata K, Shishido T, Hanafusa H.** v-Crk activates the phosphoinositide 3-kinase/AKT pathway by utilizing focal adhesion kinase and H-Ras. *Mol Cell Biol* 22: 7015–7023, 2002.
3. **Barry ST, Flinn HM, Humphries MJ, Critchley DR, Ridley AJ.** Requirement for Rho in integrin signalling. *Cell Adhes Commun* 4: 387–398, 1997.
4. **Belousov VV, Fradkov AF, Lukyanov KA, Staroverov DB, Shakhbazov KS, Terskikh AV, Lukyanov S.** Genetically encoded fluorescent indicator for intracellular hydrogen peroxide. *Nat Methods* 3: 281–286, 2006.
5. **Ben Mahdi MH, Andrieu V, Pasquier C.** Focal adhesion kinase regulation by oxidative stress in different cell types. *IUBMB Life* 50: 291–299, 2000.
6. **Beningo KA, Dembo M, Kaverina I, Small JV, Wang YL.** Nascent focal adhesions are responsible for the generation of strong propulsive forces in migrating fibroblasts. *J Cell Biol* 153: 881–888, 2001.
7. **Brown DI, Lassegue B, Lee M, Zafari R, Long JS, Saavedra HI, Griendling KK.** Poldip2 knockout results in perinatal lethality, reduced cellular growth and increased autophagy of mouse embryonic fibroblasts. *PLoS One* 9: e96657, 2014.
8. **Butler JP, Tolic-Norrelykke IM, Fabry B, Fredberg JJ.** Traction fields, moments, and strain energy that cells exert on their surroundings. *Am J Physiol Cell Physiol* 282: C595–C605, 2002.
9. **Chen HC, Appeddu P, Isoda H, Guan JL.** Phosphorylation of tyrosine 397 in focal adhesion kinase is required for binding phosphatidylinositol 3-kinase. *J Biol Chem* 271: 26329–26334, 1996.
10. **Chiarugi P, Pani G, Giannoni E, Taddei L, Colavitti R, Raugei G, Symons M, Borrello S, Galeotti T, Ramponi G.** Reactive oxygen species as essential mediators of cell adhesion: the oxidative inhibition of a FAK tyrosine phosphatase is required for cell adhesion. *J Cell Biol* 161: 933–944, 2003.
11. **Chikumi H, Fukuhara S, Gutkind JS.** Regulation of G protein-linked guanine nucleotide exchange factors for Rho, PDZ-RhoGEF, and LARG by tyrosine phosphorylation. *J Biol Chem* 277: 12463–12473, 2002.
12. **Clempus RE, Sorescu D, Dikalova AE, Pounkova L, Jo P, Sorescu GP, Schmidt HH, Lassegue B, Griendling KK.** Nox4 is required for maintenance of the differentiated vascular smooth muscle cell phenotype. *Arterioscler Thromb Vasc Biol* 27: 42–48, 2007.
13. **Datla SR, Peshavariya H, Dusting GJ, Mahadev K, Goldstein BJ, Jiang F.** Important role of Nox4 type NADPH oxidase in angiogenic responses in human microvascular endothelial cells in vitro. *Arterioscler Thromb Vasc Biol* 27: 2319–2324, 2007.
14. **Del Re DP, Miyamoto S, Brown JH.** Focal adhesion kinase as a RhoA-activable signaling scaffold mediating Akt activation and cardiomyocyte protection. *J Biol Chem* 283: 35622–35629, 2008.
15. **Ezratty EJ, Partridge MA, Gundersen GG.** Microtubule-induced focal adhesion disassembly is mediated by dynamin and focal adhesion kinase. *Nat Cell Biol* 7: 581–590, 2005.
16. **Giannoni E, Buricchi F, Raugei G, Ramponi G, Chiarugi P.** Intracellular reactive oxygen species activate Src tyrosine kinase during cell adhesion and anchorage-dependent cell growth. *Mol Cell Biol* 25: 6391–6403, 2005.
17. **Gozin A, Franzini E, Andrieu V, Da Costa L, Rollet-Labelle E, Pasquier C.** Reactive oxygen species activate focal adhesion kinase, paxillin and p130cas tyrosine phosphorylation in endothelial cells. *Free Radic Biol Med* 25: 1021–1032, 1998.
18. **Hanna IR, Hilenski LL, Dikalova A, Taniyama Y, Dikalov S, Lyle A, Quinn MT, Lassegue B, Griendling KK.** Functional association of nox1 with p22phox in vascular smooth muscle cells. *Free Radic Biol Med* 37: 1542–1549, 2004.
19. **Haurani MJ, Cifuentes ME, Shepard AD, Pagano PJ.** Nox4 oxidase overexpression specifically decreases endogenous Nox4 mRNA and inhibits angiotensin II-induced adventitial myofibroblast migration. *Hypertension* 52: 143–149, 2008.
20. **Heidkamp MC, Bayer AL, Scully BT, Eble DM, Samarel AM.** Activation of focal adhesion kinase by protein kinase Cε in neonatal rat ventricular myocytes. *Am J Physiol Heart Circ Physiol* 285: H1684–H1696, 2003.
21. **Hilenski LL, Clempus RE, Quinn MT, Lambeth JD, Griendling KK.** Distinct subcellular localizations of Nox1 and Nox4 in vascular smooth muscle cells. *Arterioscler Thromb Vasc Biol* 24: 677–683, 2004.
22. **Jurado C, Haserick JR, Lee J.** Slipping or gripping? Fluorescent speckle microscopy in fish keratocytes reveals two different mechanisms for generating a retrograde flow of actin. *Mol Biol Cell* 16: 507–518, 2005.
23. **Kumagai N, Morii N, Fujisawa K, Nemoto Y, Narumiya S.** ADP-ribosylation of rho p21 inhibits lysophosphatidic acid-induced protein tyrosine phosphorylation and phosphatidylinositol 3-kinase activation in cultured Swiss 3T3 cells. *J Biol Chem* 268: 24535–24538, 1993.
24. **Lauffenburger DA, Horwitz AF.** Cell migration: a physically integrated molecular process. *Cell* 84: 359–369, 1996.
25. **Lee CF, Ullevig S, Kim HS, Asmis R.** Regulation of Monocyte Adhesion and Migration by Nox4. *PLoS One* 8: e66964, 2013.
26. **Lombardi ML, Knecht DA, Dembo M, Lee J.** Traction force microscopy in Dictyostelium reveals distinct roles for myosin II motor and

actin-crosslinking activity in polarized cell movement. *J Cell Sci* 120: 1624–1634, 2007.
27. **Lyle AN, Deshpande NN, Taniyama Y, Seidel-Rogol B, Pounkova L, Du P, Papaharalambus C, Lassegue B, Griendling KK.** Poldip2, a novel regulator of Nox4 and cytoskeletal integrity in vascular smooth muscle cells. *Circ Res* 105: 249–259, 2009.
28. **Mackay DJG, Hall A.** Rho GTPases. *J Biol Chem* 273: 20685–20688, 1998.
29. **Markvicheva KN, Bogdanova EA, Staroverov DB, Lukyanov S, Belousov VV.** Imaging of intracellular hydrogen peroxide production with HyPer upon stimulation of HeLa cells with epidermal growth factor. *Methods Mol Biol* 476: 79–86, 2008.
30. **McGrail DJ, Kieu QM, Dawson MR.** The malignancy of metastatic ovarian cancer cell is increased on soft matrices through a mechanosensitive Rho/ROCK pathway. *J Cell Sci* 127: 2621–2626, 2014.
31. **Meng D, Lv DD, Fang J.** Insulin-like growth factor-I induces reactive oxygen species production and cell migration through Nox4 and Rac1 in vascular smooth muscle cells. *Cardiovasc Res* 80: 299–308, 2008.
32. **Meng TC, Fukada T, Tonks NK.** Reversible oxidation and inactivation of protein tyrosine phosphatases in vivo. *Mol Cell* 9: 387–399, 2002.
33. **Möhl C, Kirchgessner N, Schäfer C, Hoffmann B, Merkel R.** Quantitative mapping of averaged focal adhesion dynamics in migrating cells by shape normalization. *J Cell Sci* 125: 155–165, 2012.
34. **Munevar S, Wang Y, Dembo M.** Traction force microscopy of migrating normal and H-ras transformed 3T3 fibroblasts. *Biophys J* 80: 1744–1757, 2001.
35. **Nalbant P, Chang YC, Birkenfeld J, Chang ZF, Bokoch GM.** Guanine nucleotide exchange factor-H1 regulates cell migration via localized activation of RhoA at the leading edge. *Mol Biol Cell* 20: 4070–4082, 2009.
36. **Nobes CD, Hall A.** Rho GTPases control polarity, protrusion, and adhesion during cell movement. *J Cell Biol* 144: 1235–1244, 1999.
37. **Pan Q, Qiu WY, Huo YN, Yao YF, Lou MF.** Low levels of hydrogen peroxide stimulate corneal epithelial cell adhesion, migration, and wound healing. *Invest Ophthalmol Vis Sci* 52: 1723–1734, 2011.
38. **Pathak A, Kumar S.** Independent regulation of tumor cell migration by matrix stiffness and confinement. *Proc Natl Acad Sci USA* 109: 10334–10339, 2012.
39. **Pelham RJ Jr, Wang Y.** Cell locomotion and focal adhesions are regulated by substrate flexibility. *Proc Natl Acad Sci USA* 94: 13661–13665, 1997.
40. **Pertz O, Hodgson L, Klemke RL, Hahn KM.** Spatiotemporal dynamics of RhoA activity in migrating cells. *Nature* 440: 1069–1072, 2006.
41. **Raftopoulou M, Hall A.** Cell migration: Rho GTPases lead the way. *Dev Biol* 265: 23–32, 2004.
42. **Rape A, Guo Wh, Wang Yl.** Microtubule depolymerization induces traction force increase through two distinct pathways. *J Cell Sci* 124: 4233–4240, 2011.
43. **Reyes CD, Garcia AJ.** A centrifugation cell adhesion assay for high-throughput screening of biomaterial surfaces. *J Biomed Mater Res A* 67: 328–333, 2003.
44. **Ridley AJ.** Rho GTPases and cell migration. *J Cell Sci* 114: 2713–2722, 2001.
45. **Ridley AJ, Schwartz MA, Burridge K, Firtel RA, Ginsberg MH, Borisy G, Parsons JT, Horwitz AR.** Cell migration: Integrating signals from front to back. *Science* 302: 1704–1709, 2003.
46. **Samarakoon R, Higgins CE, Higgins SP, Higgins PJ.** Differential requirement for MEK/ERK and SMAD signaling in PAI-1 and CTGF expression in response to microtubule disruption. *Cell Signal* 21: 986–995, 2009.
47. **San Martin A, Griendling KK.** Redox control of vascular smooth muscle migration. *Antioxid Redox Signal* 12: 625–640, 2010.
48. **Torsoni AS, Marin TM, Velloso LA, Franchini KG.** RhoA/ROCK signaling is critical to FAK activation by cyclic stretch in cardiac myocytes. *Am J Physiol Heart Circ Physiol* 289: H1488–H1496, 2005.
49. **Vepa S, Scribner WM, Parinandi NL, English D, Garcia JGN, Natarajan V.** Hydrogen peroxide stimulates tyrosine phosphorylation of focal adhesion kinase in vascular endothelial cells. *Am J Physiol Lung Cell Mol Physiol* 277: L150–L158, 1999.
50. **Wang JH, Lin JS.** Cell traction force and measurement methods. *Biomech Model Mechanobiol* 6: 361–371, 2007.
51. **Zhai J, Lin H, Nie Z, Wu J, Canete-Soler R, Schlaepfer WW, Schlaepfer DD.** Direct interaction of focal adhesion kinase with p190RhoGEF. *J Biol Chem* 278: 24865–24873, 2003.